Optim Eng
https://doi.org/10.1007/s11081-018-9382-9

Intelligent secondary control in smart microgrids: an on-line approach for islanded operations

Shoresh Shokoohi[1] · Sajjad Golshannavaz[2] · Rahmat Khezri[1] · Hassan Bevrani[1]

Received: 13 December 2016 / Revised: 3 August 2017 / Accepted: 10 March 2018

Abstract Dealing with islanded microgrids (MGs), this paper aims at improving the secondary control process to restrict the fluctuations in both the voltage and frequency signals. With the aim of retrieving these parameters at the nominal values, an intelligent control scheme is devised to adjust the corresponding control parameters. To do so, an on-line self-optimizing control approach is embedded in the MG's central controller. In the tuning process, evolutionary-based techniques such as genetic algorithms provide proper initial adjustment for the parameters. Subsequently, an artificial neural network (ANN) is triggered to provide accurate online modification of the control parameters. Specifically, the training capability of the ANN mechanism along with its extensibility feature avoids the dependency of the controller on the operating point conditions and accommodates different changes and uncertainty reflections. Detailed simulation studies are conducted to investigate the performance of the proposed approach, and the results are discussed in depth.

Keywords Microgrid (MG) · Distributed generation (DG) · Intelligent secondary voltage and frequency controller · Artificial neural networks (ANNs) · Self-optimizing on-line controller

✉ Sajjad Golshannavaz
s.golshannavaz@urmia.ac.ir

[1] Electrical Engineering Department, University of Kurdistan, Sanandaj, Iran

[2] Electrical Engineering Department, Urmia University, Urmia, Iran

1 Introduction

The recent technological revolution in power systems has stimulated substantial transitions toward modern, smart, and sustainable grids. Microgrids (MGs), as such newly emergent small-scale grids, can accommodate various technologies, including power electronics devices, renewable energy resources, energy storage, and demand-response programs. The inclusion of two-way communication between these ingredients and the MG's central controller (MGCC) has facilitated the implementation of well-defined control strategies. Accordingly, efficient control processes such as active/reactive power control, voltage/frequency regulation, and energy management loops are implemented in MGCC. In addition to the grid-connected mode, these small-scale grids are able to operate in off-grid or so-called islanded mode. In both of these operating modes, the presence of various technologies, uncertainties in renewable generations, and the physical disturbances highlight the need for intelligent and robust control structures to ensure the technical and economical performance (Fathi and Bevrani 2013).

With the aim of providing the required control actions, a hierarchical control process is proposed by Bevrani et al. (2012a). In this context, the implemented controller contains two main subcontrollers: microsource controllers (MCs) and load controllers (LCs). The MCs are local modules, implanted on distributed generations (DGs), to monitor and control the voltage and frequency signals. Meanwhile, the control of the controllable load is accomplished by the LC. Moreover, an emergency controller is introduced to accurately identify possible contingencies and determine appropriate countermeasures. At higher levels of automation, the MGCC feeds the distribution management system with the required data. Thus, safe operation of MG is ensured in grid-connected mode. It also receives the propagated control commands through the distribution network operator. From another point of view, three control layers are deployed in MGCC. In this way, primary/local, supplementary/secondary, and global/tertiary controllers are used. A brief description of each layer is as follows. The primary controller deals with the initial steps in voltage and current control requirements, respected for each DG. Next, the supplementary controller curbs the remaining deviations at zero, and finally the global controller manages the MG operations to attain techno-economic cooperation with the main grid (Guerrero et al. 2011). Taking into account the outlined context, IEEE Standard 1547 compels the implementation of efficient active and reactive power controllers to undertake a secure operation of MGs. This standard also concerns the abilities of control mechanisms to provide suitable frequency and voltage stabilities (IEEE 2003). There are various MG control requirements, but an outfitted secondary voltage and frequency controller is a well-recognized way to preserve stable operation.

Early research into secondary MG controllers led to classical proportional-integral (PI) controllers (Khezri et al. 2015; Mishra 2009; De Brabandere et al. 2007). Simplicity and ease of implementation are the main factors in the industrial success of these controllers. However, they depend on the operating point conditions, which makes them less reliable and robust. To avoid this dependence, some researchers have established online tuning approaches. Extracting a precise mathematical model for the investigated plant leads to a sophisticated control mechanism, but obtaining a mathematical model for such systems is a challenging task (Bevrani et al. 2014; Khezri et al. 2017a). Intelligent learning algorithms provide appropriate ways to overcome the technical bottlenecks. Online and robust tuning controllers greatly enhance the secondary voltage and frequency control missions.

Being directed to the highlighted research line, online and intelligent controllers are deployed to perform the secondary control processes for islanded MGs (Bevrani et al. 2012b, c; Khezri et al. 2017b; Shokoohi et al. 2014). In these surveys, intelligent systems, including fuzzy logic (FL) and particle swarm optimization, are investigated for optimal tuning of conventional controllers. Artificial neural networks (ANNs) are applied in a similar manner; the details of ANN-based controllers are discussed in Shokoohi et al. (2014). In this approach, the parameters of the PI controller are simultaneously tuned based on online measurements. Such measurements are readily available given the two-way communication. The proposed controller gives a better response, but its learning process may be impacted by imperfect input data. Thus, robust performance is not guaranteed for all the operating points. The possibility of using an optimization process has been overlooked in the previous surveys. Moreover, although the implemented control structures improve either the voltage or the frequency control, the simultaneous control of these parameters has not been achieved (Bevrani et al. 2012c; Shokoohi et al. 2014). The proposed approaches are not concerned with simultaneous improvements in the voltage and frequency deviations. In other words, there is currently no online intelligent simultaneous voltage and frequency control approach that is capable of providing robust and finely tuned control.

The present study establishes an efficient control process encompassing inner, droop, and secondary controllers to improve the MG's overall performance. The proposed approach is adopted for the automatic and simultaneous adjustment of voltage and frequency signals in the MG assembly. As a starting point, the controller parameters are tuned based on a genetic algorithm (GA) in an offline fashion. This stage is in fact the first step toward an optimal controller. Next, with the aim of suppressing possible deviations in the voltage and frequency signals, a self-tuning online ANN mechanism is developed for the optimal tuning of the controller parameters. The learning capability of the ANN controller greatly improves the extensibility features of the proposed control mechanism, and hence a generalized and independent online controller is achieved. In summary, the main contributions of the present study are:

- We highlight the importance of optimal online simultaneous secondary control of voltage and frequency in MGs;
- We develop an initial GA-based approach for partial simultaneous tuning of the controller;
- We establish a robust and online fine-tuning approach based on the ANN learning features to handle the loading variations.

The remainder of this manuscript is organized as follows. Section 2 describes the proposed control structure. The GA-based offline tuning approach for the controller parameters is presented in Sect. 3. Then in Sect. 4, the proposed controller is developed into an online ANN-based MGCC to simultaneously curb the fluctuations in the voltage and frequency signals. Extensive simulation studies are conducted in Sect. 5 to analyze the performance of the proposed controller. Section 6 concludes the paper.

2 Control structures

2.1 Power and inner control loops

Consider an islanded MG as depicted in Fig. 1a. This system has three phases, including three inverter-interfaced distributed generations (IIDGs) with ratings of 220 V and 50 Hz. Two units of load banks are available in the system (Bevrani and Shokoohi 2013). For the IIDGs, Fig. 1b demonstrates the corresponding control structures in which all of the measured signals are represented in a d-q rotating frame. The power electronics stage is composed of an inverter, a PWM generator, an output filtering stage, and an interfacing inductor. Given the fast dynamics of inverters, the DC side voltage is regarded as an ideal source. Thus, its dynamics is safely passed over (Hatziargyriou et al. 2000).

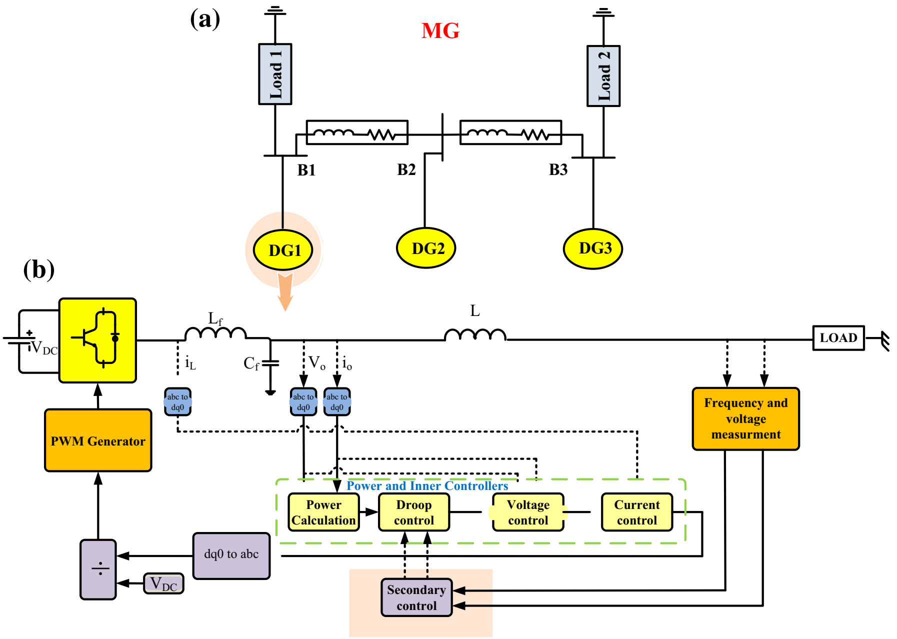

Fig. 1 **a** An islanded MG including three IIDGs; **b** the implemented control mechanism for each IIDG

There are different controllers adopted as power, voltage, and current control loops, which are shown in Fig. 2a–c, respectively. Taking into account the droop mechanisms, namely the P/f and Q/V characteristics, the power controller adjusts the voltage magnitude and the frequency at the reference points. As shown, m and n are the conventional frequency and voltage droop coefficients. In order to eliminate the instantaneous fluctuations, the instantaneous active and reactive power components are passed through low-pass filters with cut-off frequency ω_c. However, these controllers may lose their acceptable performance in some situations. If the line's impedance, connecting the IIDG to the load bank, comprises a significant resistive component, proper control action may be lost (Ahmadi et al. 2015). Since the MGCC observes the whole MG in an online fashion, the secondary control loops avoid such conditions. If the reference value is set to zero for the q-axis, the output voltage magnitude includes only the d-axis component. Although the main issues are discussed here, interested readers are referred to Bevrani (2014) for detailed information on the MG modeling. As mentioned earlier, the inner voltage and current controllers are shown in Fig. 2b, c. As can be seen, the reference points for both the voltage and current magnitudes are tracked based on two PI controllers. Feedforward components are included to enhance the controller performance under transient conditions and to compensate for the dynamic couplings between the d and q axes (Marwali and Keyhani 2004).

2.2 Secondary controllers

The main duty of the secondary controller is to mitigate the steady-state errors that are not compensated for by the droop controllers. The implemented secondary

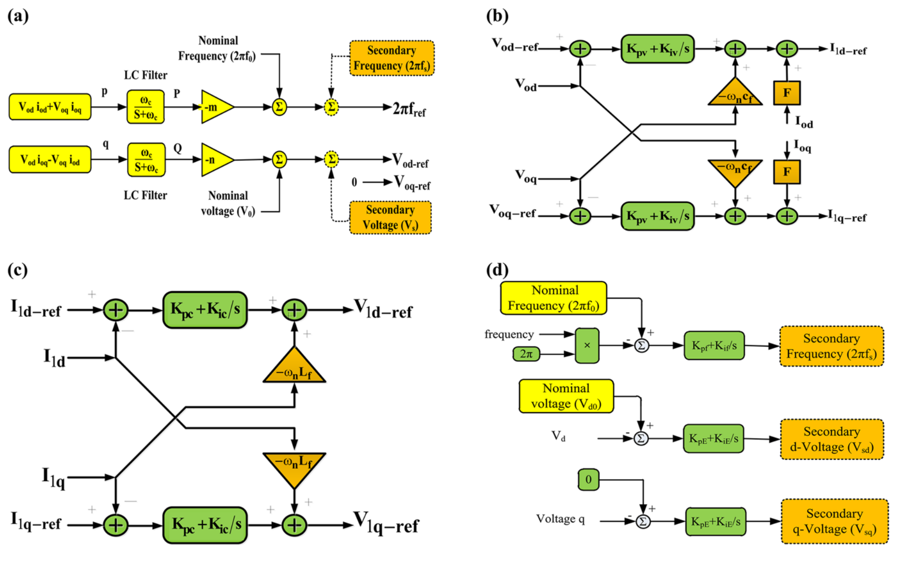

Fig. 2 Schematic representation of **a** power controller, **b** inner voltage controller, **c** inner current controller, and **d** secondary voltage and frequency controllers

voltage and frequency controllers are shown in Fig. 2d. Herein, k_{pf}, k_{if}, k_{pE}, and k_{iE} are the PI controller parameters. As mentioned earlier, the frequency signal is directly measured and then compared with its nominal value. Then, the signal released by the corresponding PI controller is suitably supplemented by the power controller. A similar practice is applied in the voltage control process. Having selected proper parameters for the PI controllers, we tune them to successfully minimize the deviations in the voltage signal. The secondary controller concerns the voltage and frequency deviations on the load side and generates an auxiliary additive signal to be supplemented on the control set-points of each DG. It should be noted that the control signals from the secondary control do not change the reference points and only modify them slightly. In other words, they supplement the set-points determined through the primary control. Accordingly, to mitigate the load voltage and frequency deviations, effective measurements are conducted after the interfacing inductance on the load side. It can be deduced that the secondary controllers are one of the major control processes in the MG assembly, contributing to safe operation. However, such impressive effects require careful attention to the efficient design of the secondary controllers.

3 Offline tuning of control parameters using GA

As clarified, each IIDG requires two inner voltage and current controllers along with two secondary loops accommodating the voltage and frequency signals. Each controller contains two control parameters: proportional (k_P) and integral (k_I) coefficients. Therefore, there are eight control parameters represented by $[k_{pv}\ k_{iv}\ k_{pc}\ k_{ic}\ k_{pE}\ k_{iE}\ k_{pf}\ k_{pf}]$. Various mathematical methods such as robust and model-based techniques can be used to tune these parameters (Bevrani et al. 2015). However, these approaches require the extraction of a precise mathematical model for the investigated plant. This is generally a complicated and time-consuming task. What is more, the changing conditions and different variations of the power system mean that there is no fixed mathematical model for all system conditions (Etemadi et al. 2012). The use of evolutionary algorithms such as GAs alleviates most of these concerns and makes it possible to tune the parameters over a wider operating range. GAs are flexible enough to operate on numerous strings simultaneously, where each string represents a different solution to a given problem. Thus, a careful scan of the search space is performed. The possibility of getting stuck at a local minimum is greatly decreased, and the results are associated with higher confidence levels (Tiwari and Vidyarthi 2000). Hence, we use a GA as the optimization engine. The GA was first explored by Holland (1975) and then by several researchers including Rechenberg et al. (1973), Schwefel (1977), and Fogel and Fogel (1994). More details of the GA mechanism can be found in Goldberg and Holland (1988).

For the sake of simplicity, we set all eight parameters to the same values for all the IIDGs. When we apply the GA to the investigated system, the search space is initially limited. Based on knowledge of the control parameter ranges in the investigated MG, we define a suitable range to provide proper freedom for the GA and result in a satisfactory control process. Accordingly, the minimum and maximum limits for each control parameter are set to 0 and 1000 respectively. The proposed chromosome is a string including eight genes for the corresponding parameters. To adjust the voltage and frequency signals at the rated values, we use the following objective function:

$$f_{object} = \sqrt{\sum_{i=1}^{K}\left[\left[\sum_{n=1}^{N=t\times k_{sc}} \Delta v_i^2(n)\right] + K_f \times \left[\sum_{n=1}^{N=t\times k_{sc}} \Delta f_i^2(n)\right]\right]} \tag{1}$$

where Δv_i and Δf_i are respectively the voltage and frequency deviations in $\mathrm{IIDG_i}$; K and N are the number of IIDGs and the number of samples in simulation time t, respectively. As well, a scaling coefficient of k_{sc} (equal to 10^5) is included to represent the simulation time. In a low-voltage distribution system, i.e., 220 V and 50 Hz, the upper limits of the voltage and frequency deviations are respectively set to 5 and 1% of their nominal values. Therefore, the maximum deviations are 11 V (0.05 $\times$ 220) for the voltage and 0.5 Hz (0.01 $\times$ 50) for the frequency. It can easily be observed that the maximum deviation of the voltage signal is 22 times greater than that of the frequency signal (11/0.5 = 22). Hence, to assign equal weights for the voltage and frequency deviations, the coefficient K_f is selected as $22^2 = 484 \approx 500$. To give precise tuning of the control parameters, we apply different loading states to the examined MG. These states are represented in Table 1. In the interval $t \in (0, 0.5)$ s, load banks 1 and 2 are resistive and resistive-inductive, respectively. After $t = 0.5$ s and for the next nine steps, active, reactive, and capacitive loads are deployed. Because sudden changes in the loading conditions could intensify the system instability, we consider such variations in the numerical studies. Considering (1) and the corresponding coefficients defined earlier, the GA performs optimal tuning of the control parameters. Figure 3 gives a flowchart for the proposed approach. It can be seen that following an initialization stage, the initial control

Table 1 Load change scenarios

Time intervals (s)	Load 1	Load 2
0.0–0.5	50 Ω	100 Ω + 200 mH
0.5–1.0	500 Ω + 500 mH	100 Ω + 200 mH
1.0–1.5	500 Ω + 500 mH	50 Ω + 100 μH
1.5–2.0	20 Ω + 100 μH	50 Ω + 100 μH
2.0–2.5	20 Ω + 100 μH	50 Ω + 100 mH
2.5–3.0	500 Ω + 200 mH + 10 μF	50 Ω + 100 mH
3.0–3.5	500 Ω + 200 mH + 10 μF	500 Ω
3.5–4.0	10 Ω + 1 mH + 20 μF	500 Ω
4.0–4.5	10 Ω + 1 mH + 20 μF	10 Ω + 20 mH + 100 μF
4.5–5.0	100 Ω	10 Ω + 20 mH + 100 μF

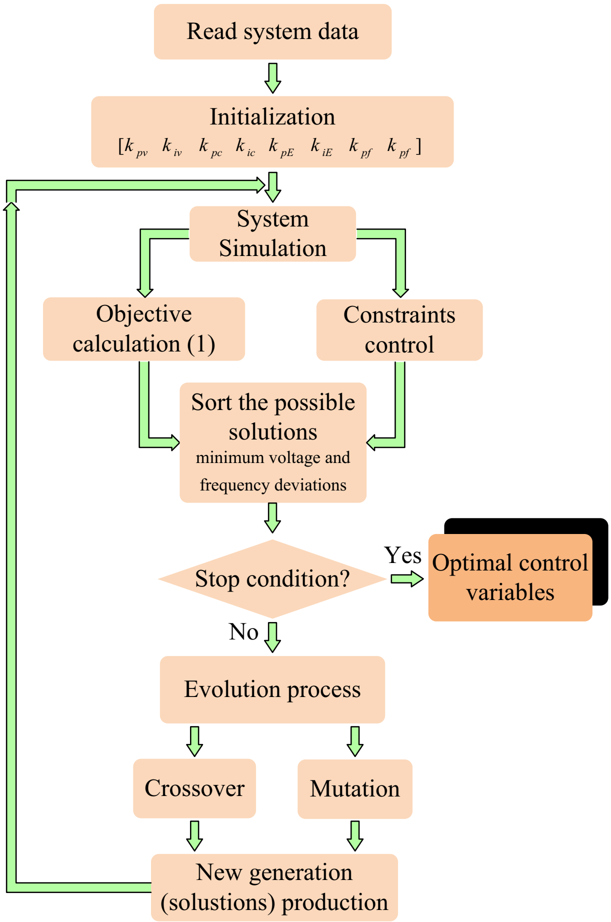

Fig. 3 Flowchart of the proposed optimization process based on GA

parameters are evaluated and their performance is tailored based on the objective function. Then, the population is sorted to find the minimum voltage and frequency deviations, based on which crossover and mutation operators are deployed to produce a new population or generation. Once the termination criterion is reached, the optimal control parameters are determined.

Figure 4 shows the convergence curve obtained for the investigated system. As can be seen, the problem converges to its optimal value. Thus, the optimal control parameters are attained, which are listed in Table 2. Note that since this stage is the initial offline stage of the proposed approach, a short convergence time is not important, and longer times could lead to better control parameters.

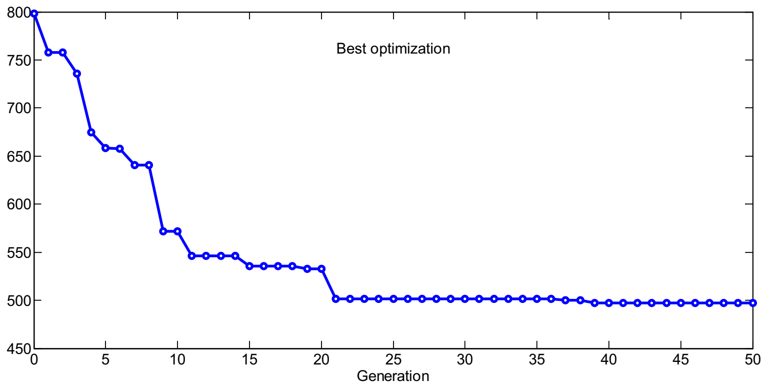

Fig. 4 Convergence curve for the investigated system

Table 2 Optimal values of control parameters

Parameter	Optimal value
k_{pv}	0.96
k_{pc}	884.02
k_{pE}	0.02
k_{pf}	0.25
k_{iv}	466.67
k_{ic}	3814.88
k_{iE}	1.34
k_{if}	1.95

4 Proposed online intelligent tuning of control parameters

As explained earlier, following changes in the loading conditions or generating units, secondary controllers would be triggered to suppress the voltage and frequency deviations. The initial stage in tuning the control parameters is performed based on GA operators in an offline manner. Its performance has been discussed in the previous sections. However, if the operating point varies greatly, ensuring an optimal response is a challenging task. To improve the capability of the secondary controllers, we apply intelligent and evolutionary algorithms to obtain a fine and online tuning of the control parameters (Bevrani and Hiyama 2011). A brief review of the available literature reveals that current methods are effective only for voltage or frequency regulations and not for simultaneous tuning. However, simultaneous voltage and frequency control is important to ensure the successful and reliable operation of MGs. We therefore develop an ANN-based controller that is in direct contact with the GA optimization. Specifically, the ANN is a parallel computational platform that includes numerous processing components. To fulfill a particular mission, these components are put into a particular arrangement. Its advantages include parallel computation, extensibility, and tolerable mechanisms for the uncertain and noisy processes. In general, two methods are used to update the weights and the training process: feedforward and feedback. Feedback processes include supervised, unsupervised, and reinforcement approaches. For more information, see Gupta et al. (2004), Hagan et al. (1996).

Because of DG outages or loading variations, the operating point of the MG varies. Thus, considerable deviations are observed in the voltage and frequency signals. The initial control parameters that are tuned by the GA require further corrections to preserve the nominal set-points. If the control action is not effective, there could be a collapse of the MG voltage and frequency. To avoid this, we use an ANN-based MGCC, depicted in Fig. 5a, to correct the control parameters. The proposed ANN controller tunes the control parameters in an online manner and extends the validity of the proposed approach to a wider range of operating conditions. A schematic representation of this system is given in Fig. 5b. As can be seen, the overall voltage and frequency deviations are gathered in the investigated system. These data are treated as the inputs to the ANN controller, and the corresponding ANN weights are updated via suitable learning rules. Thus, proper set-points are generated and transferred to each IIDG. In this way, a safe control operation is achieved that ensures the stability of the MG voltage and frequency.

Developing a mathematical representation of the ANN is a prerequisite to optimize the MGCC performance. A neuron is the key building block of each ANN structure, and it has three main components: the weights, denoted by $W_j = [w_1\ w_2 \cdots w_n]$, the bias θ, and the activation function $f(net)$. The input data are labeled x_j. The relation between these parameters is given by Eq. (2). In this equation, each input data is considered with its corresponding weight, and θ is augmented to the activation function $y(k)$ (Sarangapani 2006).

$$y(k) = f\left(\sum_{j=1}^{n} w_j x_j(k) + \theta\right) \tag{2}$$

Various functions such as logsigmoid, sign, and tansigmoid could be used as activation functions. In the learning phases of an ANN, the learning mechanism (e.g., the back-propagation approach) may require the calculation of $f'(net)$, the derivative of the activation function. If so, the activation function should be differentiable. Moreover, providing proper initial conditions for an ANN-based controller is important. The nominal values of the voltage and frequency signals are set as the desired initial values, represented by Eq. (3).

$$X_{initial} = \begin{bmatrix} 220 \\ 220 \\ 50 \\ 50 \end{bmatrix}. \tag{3}$$

An ANN-based controller has three different layers: input, output, and hidden. Typically, the number of neurons in the hidden layer is twice the number in the input. We use 10 neurons for the input layer, based on the expert's knowledge of the system. Thus, there are 20 neurons in the hidden layer. The input layer contains linear-type neurons whereas in the hidden layer, nonlinear neurons are used. The

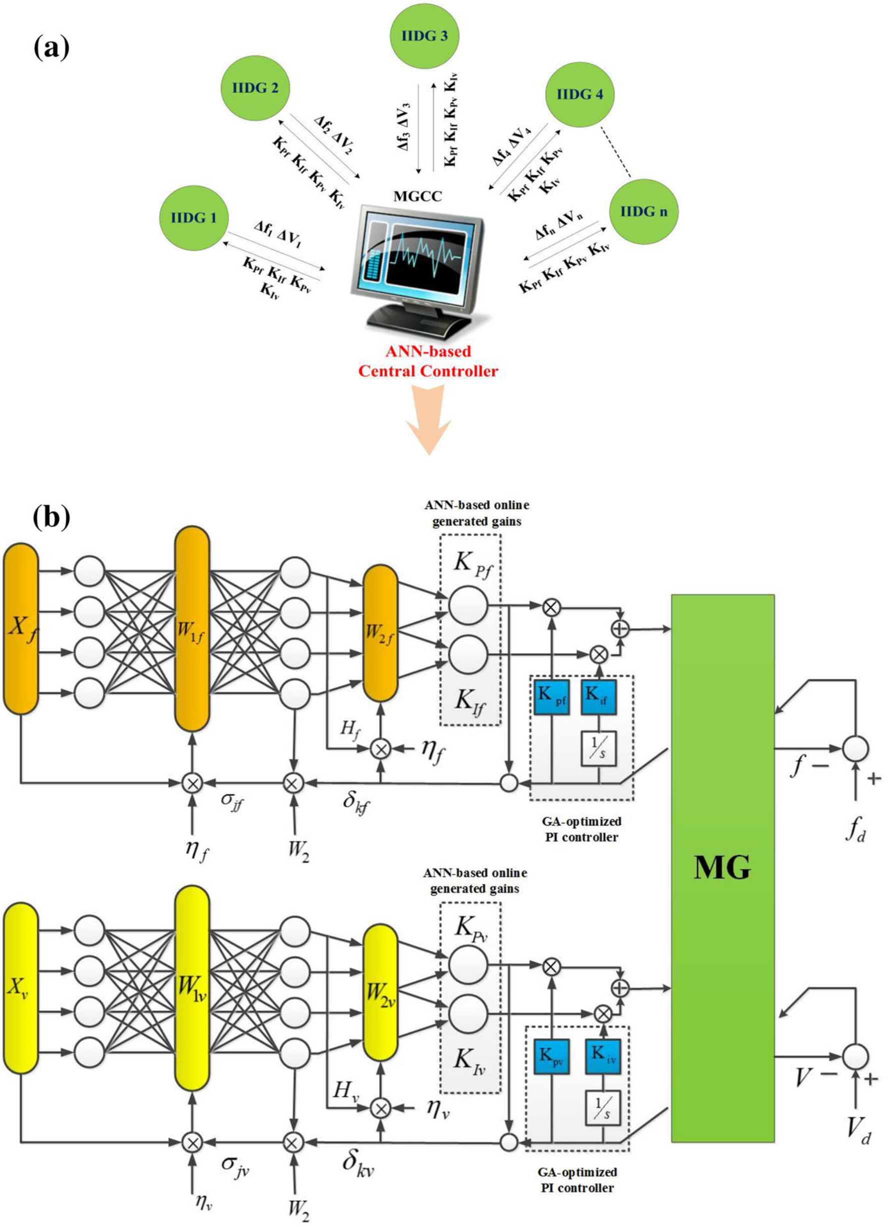

Fig. 5 **a** Overall structure of the proposed intelligent MGCC, **b** detailed representation of the GA-optimized ANN-based online approach

nonlinearity feature makes it possible to smoothly update the corresponding weights. The number of neurons in the output layer is based on the number of control variables. There are three IIDGs in the investigated MG, as shown in

Fig. 1a. Each of these IIDGs includes two secondary controllers for voltage and frequency signals. Each of these controllers contains a proportional and an integral gain. Thus, the output layer contains 12 linear neurons. W_1 represents the weight vector for the hidden layer whereas W_2 is similarly deployed for the output. Considering the feed-forward mechanism, the input vector is deployed to trigger the hidden and output layers. As clarified earlier, the main purpose behind the proposed ANN structure is to reduce the existing deviations in the voltage and frequency signals and hence improve the MG stability. To this end, the frequency and voltage outputs are compared against the desired vector, denoted by y_d. This vector includes the nominal values of the voltage and frequency signals. In this study, the supervised learning approach is used for the feedback process. The learning approach can be implemented based on the Widrow–Hoff, back-propagation, or correlation methods; we use back-propagation. Regarding the optimization goal, the proposed learning process attempts to minimize the error function:

$$e = \frac{1}{2}\sum_{i=1}^{n}(y_d - y)^2 \tag{4}$$

In this equation, the measured output variables are represented by the vector y. Subsequently, the error between the desired set-points and the measured values is calculated. The error value is then used to update the ANN weights. This process is carried out based on Eqs. (5) and (6):

$$W_2(k+1) = W_2(k) + \Delta W_2 = W_2(k) + \eta\delta_k H_j \tag{5}$$

$$W_1(k+1) = W_1(k) + \Delta W_1 = W_1(k) + \eta\sigma X \tag{6}$$

Here, ΔW_1 and ΔW_2 are the weight displacements due to the system error values. These parameters are computed based on Eqs. (7) and (8), respectively:

$$\begin{aligned}
&\Delta W_2 = -\eta\frac{\partial e}{\partial W_2}\\
&\frac{\partial e}{\partial W_2} = \frac{\partial e}{\partial y}\frac{\partial y}{\partial u}\frac{\partial u}{\partial net_k}\frac{\partial net_k}{\partial W_2}\\
&\frac{\partial net_k}{\partial W_2} = f'(net_k)\\
&\frac{\partial net_k}{\partial W_2} = H_j\\
&\frac{\partial e}{\partial y}\frac{\partial y}{\partial u}\frac{\partial u}{\partial net_k} = \delta_k\\
&\Delta W_2 = \eta\delta_k H_j
\end{aligned} \tag{7}$$

$$\begin{aligned}
\Delta W_1 &= -\eta \frac{\partial e}{\partial W_1} \\
\frac{\partial e}{\partial W_1} &= \frac{\partial e}{\partial y}\frac{\partial y}{\partial u}\frac{\partial u}{\partial net_k}\frac{\partial net_k}{\partial H_j}\frac{\partial H_j}{\partial net_j}\frac{\partial net_j}{\partial W_1} \\
\frac{\partial u}{\partial net_k} &= f'(net_k) \\
\frac{\partial net_k}{\partial H_j} &= W_2 \\
\frac{\partial H_j}{\partial net_j} &= f'(net_j) \\
\frac{\partial net_j}{\partial W_j} &= X \\
\Delta W_1 &= \eta \delta_k f'(net_k) W_2 f'(net_j) X = \eta \sigma_j X
\end{aligned} \tag{8}$$

All of the symbols in Eqs. (7) and (8) can be traced in the schematic representation of Fig. 5b. Moreover, the learning rate, which is defined as a small positive value, is denoted by η. In the proposed approach, when the error signal is below the prespecified threshold, the learning process is successfully terminated.

5 Numerical validations

To assess the performance of the proposed ANN-based GA-optimized online tuning approach, we carried out extensive numerical studies on the test system illustrated in Fig. 1a. Although the results are discussed for this specific test system, the proposed control approach is general and could be applied to other systems. MATLAB/Simulink is the simulation platform in this study. Multiple loading conditions are considered in the form of step changes to explore the dynamic response of the proposed controller. As noted in Table 3, the loading states are t = 0.3, 0.5, 0.7, 0.9, and 1.1 s. The required data regarding the IIDGs and MG branches are given in Bevrani and Shokoohi (2013). The expert's knowledge of the investigated system

Table 3 Load change scenarios

Time duration (s)	Load 1	Load 2
0–0.3	100 Ω + 200 mH	150 Ω + 100 mH + 30 μF
0.3–0.5	50 Ω + 100 mH	100 Ω + 10 μF
0.5–0.7	0	0
0.7–0.9	40 Ω + 5 μF	10 Ω + 50 μF
0.9–1.1	5 Ω + 10 mH	200 Ω + 10 mH + 150 μF
1.1–1.3	5 Ω + 10 mH	500 Ω + 10 μF

and its features impacts the selection of the neural network characteristics and the learning process and determines the selection of the weight vectors. Since the frequency and voltage signals are typically reported in these studies, they are given as the simulation results. Meanwhile, it is well understood that the active and reactive power variations are in line with the frequency and voltage variations, respectively, and result in similar waveforms. Accordingly, they are not listed in the simulation results.

Following each step change in the loading conditions, the system voltage and frequency responses are displayed in Figs. 6 and 7, respectively. In these figures, the dashed line corresponds to the offline mechanism and the solid one represents the GA-optimized ANN-based approach. The results show that the extensibility feature of the proposed ANN leads to a better response in terms of maintaining the MG's nominal values. This feature makes the ANN-based MGCC a general and online controller to accommodate a wider range of operating points with severe disturbances.

As can be seen, any change in the system operating point gives noticeable deviations in the voltage and frequency signals. Likewise, it is clear that the offline approach maintains the voltage and frequency within the permissible ranges, namely 5% for the voltage and 1% for the frequency. This approach preserves the system performance in the permissible ranges, but it yields steady-state errors around the nominal values. Moreover, if the operating point varies sensibly, as in the cases with large disturbances, this approach is likely to lose its acceptable performance. In Figs. 6 and 7, it is clear that before t = 0.9 s, the offline tuning approach returns the voltage and frequency to the nominal values. The ANN-based approach has a superior performance. However, this is not the case for the times after t = 0.9 s. During these intervals, as the intensity of the step change gets higher, this approach does not restore the system's voltage and frequency to the nominal values. In contrast, the proposed ANN-based approach demonstrates a robust and reliable operation in maintaining the secondary control missions. As can be seen, the voltage and frequency signals are regulated better than by the offline method. Thus, a generalized and robust controller is achieved for the variations in the MG's working point.

To accommodate the changes in operating points and to settle the voltage and frequency signals at the nominal values, the proposed approach manipulates the control parameters in all IIDGs. The update curves for all these parameters are shown in Figs. 8, 9 and 10. These figures reveal that the ANN-based MGCC adjusts the control parameters of all IIDGs such that the minimum fluctuations in the voltage and frequency profiles are attained.

To analyze the results in more depth, we define two indices as follows:

$$I_v = \frac{\sum_{n=1}^{N} |\Delta v|^2}{N} \tag{9}$$

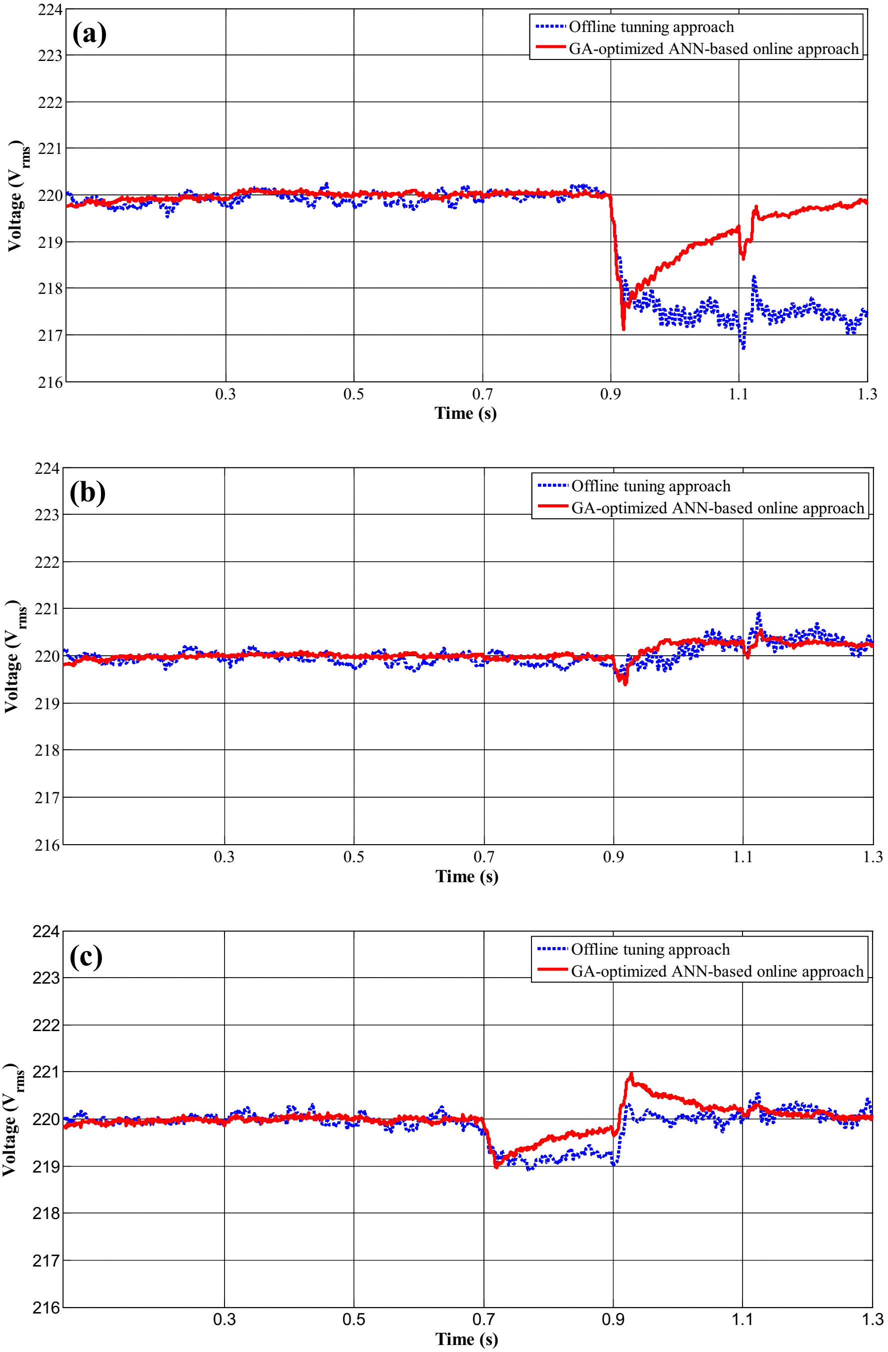

Fig. 6 Voltage profiles for the considered step changes in loading conditions: **a** IIDG1, **b** IIDG2, and **c** IIDG3

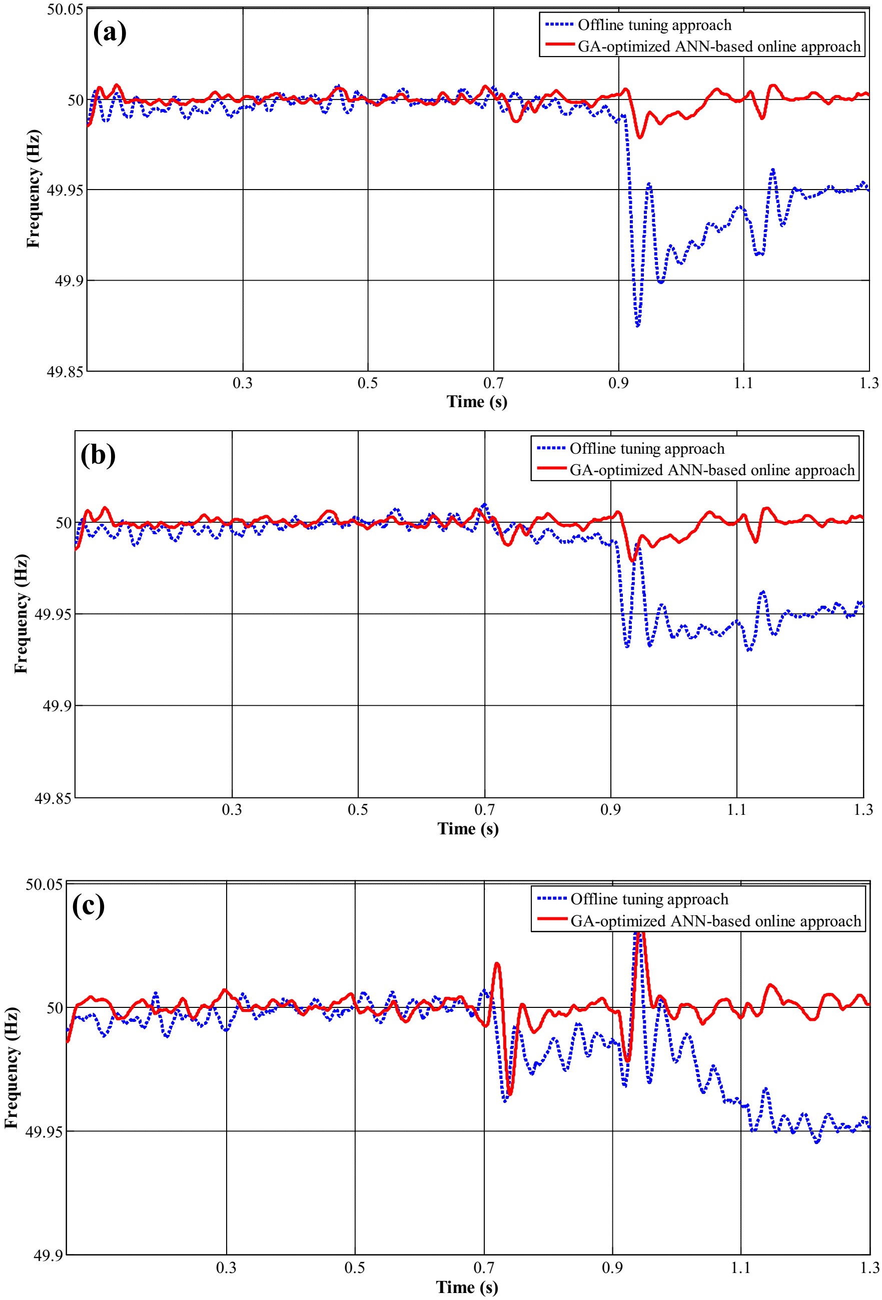

Fig. 7 Frequency profiles for the considered step changes in loading conditions: **a** IIDG1, **b** IIDG2, and **c** IIDG3

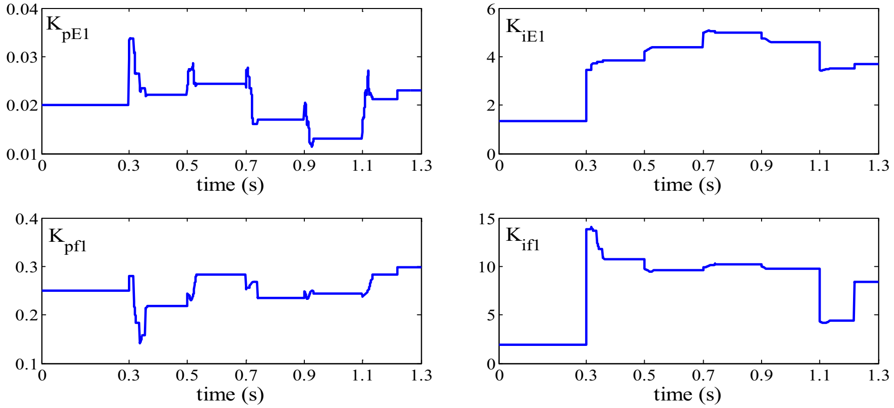

Fig. 8 Updating the secondary controller's parameters in IIDG1 following the step changes in loading conditions

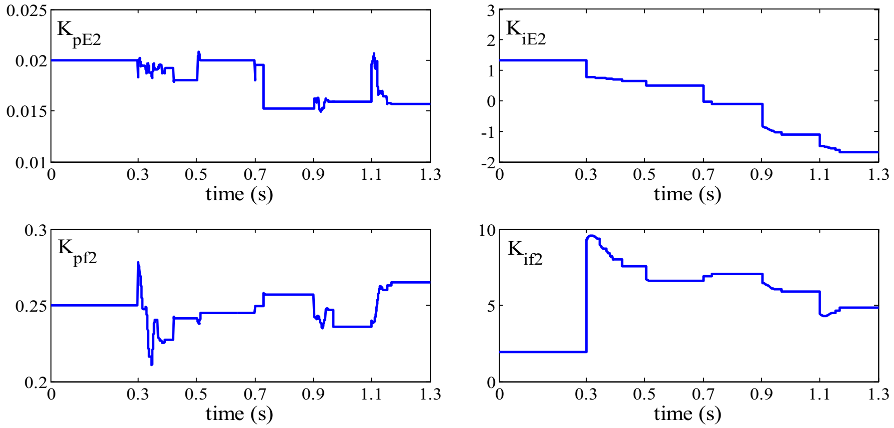

Fig. 9 Updating the secondary controller's parameters in IIDG2 following the step changes in loading conditions

$$I_f = \frac{\sum_{n=1}^{N} |\Delta f|^2}{N} \tag{10}$$

where $|\Delta v|$ and $|\Delta f|$ are the absolute values of the voltage and frequency deviations, respectively, and N is the total number of samples in the simulation time period. The performance indices are computed for the simulated scenarios introduced in Table 3. The results are reported in Table 4. Since the results are similar, we consider only IIDG1. With respect to this table, it can be deduced that the performance indices obtained based on ANN-based online approach are at least ten times smaller than the reported values for the offline approach. Thus, a more uniform steady-state operation with a minimized deviation is obtained by the proposed approach. Moreover, this approach avoids the steady-state errors observed in some

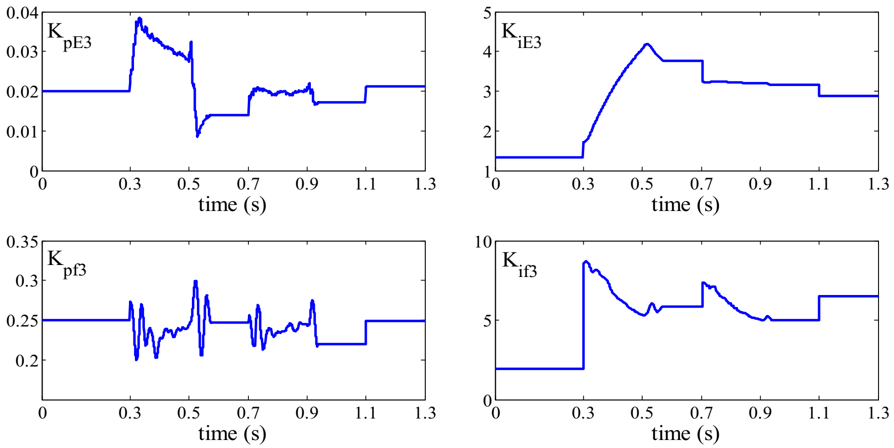

Fig. 10 Updating the secondary controller's parameters in IIDG3 following the step changes in loading conditions

Table 4 Performance indices obtained for IIDG1

Performance Index	Tuning method	
	Offline tuning approach	GA-optimized ANN-based online approach
I_v	0.4007	0.0018
I_f	0.00107	0.000109

loading scenarios. Thus, we have demonstrated the superior performance of the online ANN-based MGCC.

6 Conclusion

We have studied simultaneous secondary control in islanded MGs. When disturbances occur, the conventional PI controllers lose their ability to provide a safe operation scheme. Accordingly, the increasing deviations in both the voltage and frequency signals could steer the MG toward overall instability. On the other hand, the application of intelligent algorithms such as GA and ANN for the individual tuning of voltage or frequency does not achieve the goal of simultaneous tuning. Thus, the MG was shown to be at risk of uncontrolled operation and thus unstable conditions. In contrast, the proposed approach gives simultaneous control of secondary voltage and frequency, which greatly improves the system's operational indices. The initial tuning of the control parameters was based on a GA approach. This technique yielded improved performance of the MG, but steady state errors occurred for severe disturbances. This issue was greatly alleviated by the proposed ANN approach intended for the online fine-tuning of the control parameters. We showed that due to the extensibility and learning features of the GA-optimized ANN-based MGCC, we obtain a working-point-independent controller that greatly minimizes the emergent deviations in the voltage and frequency profiles. Thus, the steady-state errors were totally suppressed and the system operated at its nominal conditions, even when large disturbances occurred. Its ability to accommodate a wider range of operating points makes the proposed approach suitable for the successful operation of MGs.

References

Ahmadi S, Shokoohi S, Bevrani H (2015) A fuzzy logic-based droop control for simultaneous voltage and frequency regulation in an AC microgrid. Int J Electr Power Energy Syst 64:148–155

Bevrani H (2014) Robust power system frequency control, 2nd edn. Springer, Berlin

Bevrani H, Hiyama T (2011) Intelligent automatic generation control. CRC Press, Boca Raton

Bevrani H, Shokoohi S (2013) An intelligent droop control for simultaneous voltage and frequency regulation in islanded microgrids. IEEE Trans Smart Grid 4(3):1505–1513

Bevrani H, Watanabe M, Mitani Y (2012a) Microgrid controls. In: Beaty HW (ed) Standard handbook for electrical engineers, Section 16, 16th edn. McGraw Hill, New York

Bevrani H, Habibi F, Babahajyani P, Watanabe M, Mitani Y (2012b) Intelligent frequency control in an AC microgrid: online PSO-based fuzzy tuning approach. IEEE Trans Smart Grid 3(4):1935–1944

Bevrani H, Habibi F, Shokoohi S (2012c) ANN-based self-tuning frequency control design for an isolated microgrid. In: Meta-heuristics optimization algorithms in engineering, business, economics, and finance, IGI Global

Bevrani H, Watanabe M, Mitani Y (2014) Power system monitoring and control. Wiley, Hoboken

Bevrani H, Feizi MR, Ataee S (2015) Robust frequency control in an islanded microgrid: $H\infty$ and μ-synthesis approaches. IEEE Trans Smart Grids, pp 1–12

De Brabandere K, Bolsens B, Van den Keybus J, Woyte A, Driesen J, Belmans R (2007) A voltage and frequency droop control method for parallel inverters. IEEE Trans Power Electron 22(4):1107–1115

Etemadi AH, Davison EJ, Iravani R (2012) A decentralized robust control strategy for multi-DER microgrids. Part I. Fundamental concepts. IEEE Trans Power Deliv 27(4):1843–1853

Fathi M, Bevrani H (2013) Statistical cooperative power dispatching in interconnected microgrids. IEEE Trans Sustain Energy 4(3):586–593

Fogel DB, Fogel LJ (1994) Evolutionary computation. IEEE Trans Neural Netw 5(1):1–2

Goldberg DE, Holland JH (1988) Genetic algorithms and machine learning. Mach Learn 3(2):95–99

Guerrero JM, Vasquez JC, Matas J, de Vicuña LG, Castilla M (2011) Hierarchical control of droop-controlled AC and DC microgrids—a general approach toward standardization. IEEE Trans Ind Electron 58:158–172

Gupta MM, Jin L, Homma N (2004) Static and dynamic neural networks: from fundamentals to advanced theory. Wiley, New York

Hagan MT, Demuth HB, Beale MH (1996) Neural network design. Pws Pub, Boston

Hatziargyriou N, Donnelly M, Papathanassiou S, Lopes JP, Takasaki M, Chao H, Usaola J, Lasseter R, Efthymiadis A, Karoui K, Arabi S (2000) Modeling new forms of generation and storage. Cigre Technical Brochure, CIGRE TF38.01.10, pp 1–140

Holland J (1975) Adaptation in natural and artificial systems. University of Michigan Press, Ann Arbor

IEEE standard for interconnecting distributed resources with electric power systems. IEEE Std 1547-2003, pp 1–28 (2003)

Khezri R, Shokoohi S, Golshannavaz S, Bevrani H (2015) Intelligent over-current protection scheme in inverter-based microgrids. In: Smart grid conference (SGC), pp 53–59

Khezri R, Golshannavaz S, Shokoohi S, Bevrani H (2017a) Toward intelligent transient stability enhancement in inverter-based microgrids. Neural Comput Appl. https://doi.org/10.1007/s00521-017-2859-1

Khezri R, Golshannavaz S, Vakili R, Memar-Esfahani B (2017b) Multi-layer fuzzy-based under-frequency load shedding in back-pressure smart industrial microgrids. Energy 132:96–105
Marwali MN, Keyhani A (2004) Control of distributed generation systems. Part I. Voltages and currents control. IEEE Trans Power Electron 19(6):1541–1550
Mishra SK (2009) Design-oriented analysis of modern active droop-controlled power supplies. IEEE Trans Ind Electron 56:3704–3708
Rechenberg I (1994) Evolutions strategie: Optimierung technischer Systeme nach Prinzipien der biologischen Evolution. frommann-holzbog, Stuttgart, 1973. Step-size adaptation based on non-local use of selection information. In: Parallel problem solving from nature (PPSN3)
Sarangapani J (2006) Neural network control of nonlinear discrete-time systems. CRC Press, Boca Raton
Schwefel H-P (1977) Numerische Optimierung von Computer-Modellen mittels der Evolutionsstrategie: mit einer vergleichenden Einführung in die Hill-Climbing-und Zufallsstrategie. Birkhäuser, Basel
Shokoohi S, Sabori F, Bevrani H (2014) Secondary voltage and frequency control in islanded microgrids: online ANN tuning approach. In: Smart grid conference (SGC), Tehran, pp 1–6
Tiwari MK, Vidyarthi NK (2000) Solving machine loading problems in a flexible manufacturing system using a genetic algorithm based heuristic approach. Int J Prod Res 38(14):3357–3384